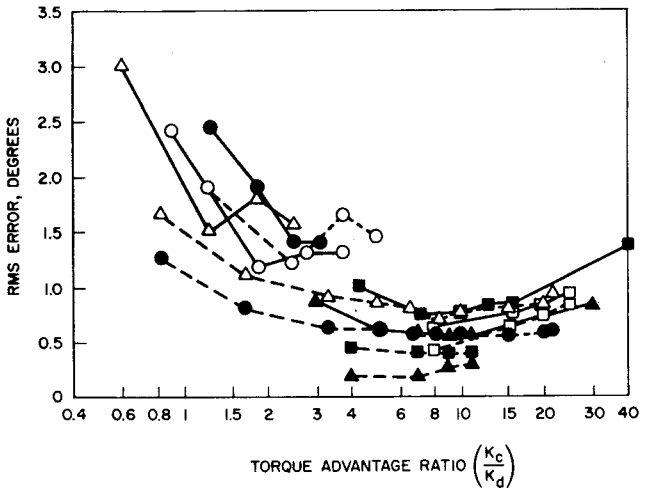

Fig. 3 Composite plot from twelve studies of the effects of TAR on rms error.

pulse characteristics as well as the amplitude and frequency characteristics of the disturbance torques. The fuel efficiency curves in Fig. 2 show knees occurring in this same TAR region. This break point was common to all of the previously mentioned system characteristics;

$$\text{fuel efficiency} = \frac{\int_0^t |\text{disturb torques}|\,dt}{\int_0^t |\text{control torques}|\,dt}$$

Figure 3 contains error plots representing more than 1000 runs from eight different experiments accomplished at Hughes and four different studies published by other agencies and companies. Most of these runs were conducted to test other system parameters but are plotted here as a function of TAR. The optimum value of TAR is near 7, with an acceptable region between 5 and 11.

Figure 4 contains a summary of the recommended angular-acceleration response for optimum handling qualities. The recommended response for free orbit, undisturbed maneuvers is indicated by the shaded region running horizontally. The CSA is expressed in degrees per second^2. The cross-hatched region running diagonally contains the recommended region for maneuvers involving disturbance torques, $5 < \text{TAR} < 11$, with the optimum at a ratio of 7. The area common to both optimum regions would indicate that a single level of acceleration response would be adequate for both disturbed and free orbit maneuvers. If the disturbance torques get too high, the optimum TAR will result in a vehicle response or CSA that is too high for optimum control during undisturbed maneuvers. This situation would indicate the need for variable or multiple levels of thrust in order to achieve satisfactory manual control.

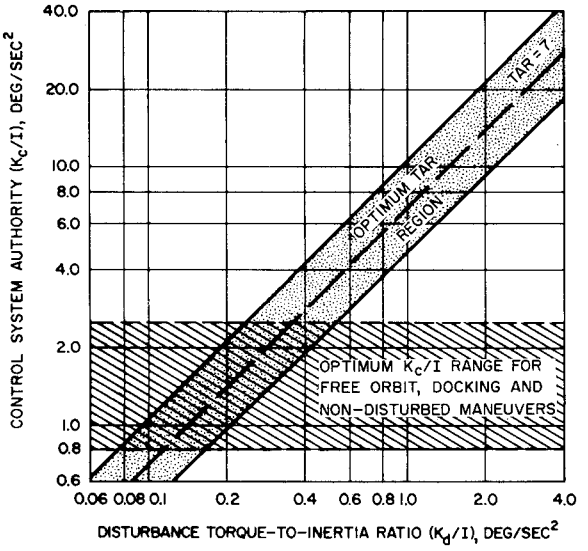

Fig. 4 Recommended angular-acceleration response for optimum handling qualities.

Conclusions

It does seem possible to describe spacecraft attitude-control systems with parameters or characteristics that will be common to all types of vehicle and mission applications. The five basic characteristics presented herein constitute an acceptable set, and they can be useful in both analysis and synthesis. The handling qualities parameters derived from these basic characteristics are critical to system effectiveness. The TAR and CSA, as defined herein, are suggested as handling qualities parameters that can be defined for all systems.

References

[1] Besco, R. O., Depolo, G. G., and Bauerschmidt, D. K., "Manual attitude control systems: Parametric and comparative studies of operating modes of control," NASA CR-56 (June 1964).

[2] Bauerschmidt, D. K. and Besco, R. O., "Human engineering criteria for manned space flight: Minimum manual systems," U. S. Air Force Wright-Patterson Air Force Base Aerospace Medical Research Lab. TDR-62-87 (1962).

[3] Montgomery, J. E., "Manned control of space vehicle docking," American Astronautical Society Paper 63-116 (September 1963).

[4] McElwain, C. S., Norris, R. E., and Besco, R. O., "Analysis and exploratory studies of docking systems for manned space vehicles," Hughes Aircraft Co. TM-749 (March 1963).

[5] Besco, R. O., "Manual attitude control systems: Display format considerations," NASA (to be published); also Hughes Aircraft Co. Rept. P64-22 (March 1964).

Experimental Heat-Transfer Study of Shock Impingement on Fins in Hypersonic Flow

W. Leon Francis*
Ford Motor Company, Newport Beach, Calif.

THE interaction of two shock waves (e.g., that generated by a vehicle with fins) may produce a flow that impinges on a vehicle surface. This localized heating will be greater than that normally predicted because of a region of high vorticity downstream of the shock intersection. To provide data pertinent to this problem, tests were made on fin-body combinations in the Jet Propulsion Laboratory (JPL) 21-in. Hypersonic Wind Tunnel. The models used were a 5° half-angle wedge body and a 6.23° cone, both with cylindrical and wedge fins in a single plane. Data on both types of fins were taken simultaneously with a single body shock generator. Tests were conducted at $M_\infty = 9$ (nominal) and $Re_\infty = 15{,}000$ and 95,000 over a range of angle of attack

Received November 11, 1964; revision received March 25, 1965. This work was supported by the U. S. Air Force through the Air Force Ballistic Systems Division, under Contract No. AF 04 (694)-23, while the author was associated with Aeronutronic, Division of Ford Motor Company in 1961.

* Aeronutronic Division. Member AIAA.

(α) to 20°; this provided a convenient method for varying the effective body geometry without constructing different half-angle bodies.

Effect of Shock Impingement on Fins

When the strengths of two intersecting shocks are considerably different, the resulting downstream flow deflections will generate discontinuities of velocity, density, and entropy, beginning at the point of intersection.[1] The entropy discontinuity theoretically will give a sheet of infinite vorticity. For a real viscous fluid, the discontinuity will not exist far downstream because the flow will immediately begin to mix, and the vorticity will diffuse into the adjacent regions. A region of large entropy gradients in the flow results. It is doubtful if a solution for the flow field can be obtained in closed form. In the situation considered here (Fig. 1), the shock wave generated by the body intersects the one standing off the fin and produces a region of high vorticity which impinges on the fin, causing a region of increased aerodynamic heating. This is somewhat analogous to the case of shock-generated vorticity at low Re. One might, therefore, use that solution as a basis for examining the shock-impingement problem. However, a fundamental difference exists between the shock-generated vorticity on a cylinder and that of the present case. In a steady two-dimensional flow with constant density, the vorticity is a function of the stream function alone, so that the vorticity at the body surface is zero. The present case thus is closer in nature to three-dimensional flow where the vorticity is nonzero on the body surface.

Hoshizaki[2] presented an approximate solution in closed form for the effect of shock-generated vorticity on three-dimensional stagnation heating in terms of quantities evaluated at the wall and immediately behind the shock wave. These results may be expressed as

$$Nu_\zeta \backsim [1 - r_s\zeta_s/r_w\zeta_w]^{-1} \qquad (1)$$

where the constant of proportionality is essentially the Nusselt number without vorticity effects. At large Re, $r_w\zeta_w$ is much greater than $r_s\zeta_s$, so that the vorticity behind the shock has little effect on the heat-transfer rate.[2] At low Re, $r_s\zeta_s/r_w\zeta_w$ is of the order of one, so that the heat-transfer rate will vary markedly depending on whether or not the shock-generated vorticity is taken into account. The numerical results confirm this. The importance of these results for the present analysis is based on an examination of the vorticity distribution in the shock layer. Calculations show a trend of increasing linearity of the vorticity profiles as the shock-vorticity effect increases. Assuming then that the vorticity distributions between shock and body are similar for the case of shock-generated vorticity and the present case of a flow discontinuity, the calculations might be interpreted to imply that as ζ_s becomes arbitrarily large, ζ_w is not only very large also but proportional to ζ_s so that the ratio ζ_s/ζ_w or Nu_ζ/Nu_0 is approximately constant. An order-of-magnitude estimate based on the indicated trends of the numerical calculations gives $Nu_\zeta/Nu_0 \simeq 5$.

If the preceding considerations are valid, the heat-transfer rates at shock impingement should be approximately constant when presented nondimensionally as a function of ζ_s. From Crocco's theorem for vorticity,

$$\zeta = [T/U][dS/dn] \qquad (2)$$

By assuming average temperatures and velocities across the discontinuity, substitution of Eq. (2) into (1) shows that temperature-velocity effects should approximately cancel, and the entropy gradient would be the appropriate correlation parameter. The actual entropy gradient is unknown, but a correlation can be obtained by considering the difference in the asymptotic entropy levels across the discontinuity

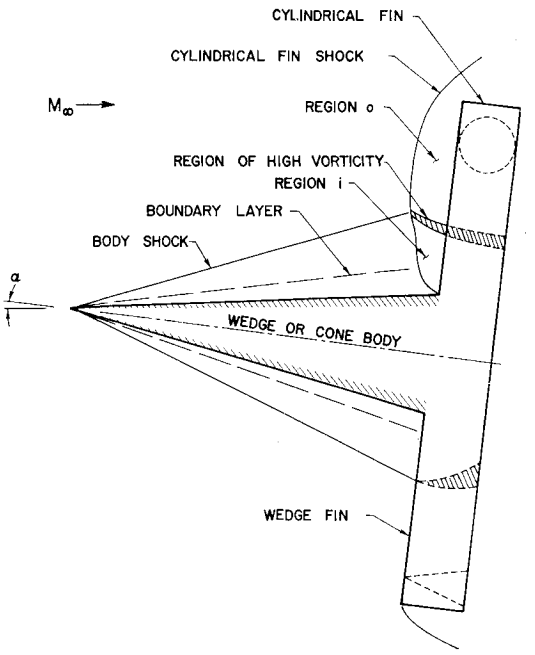

Fig. 1 Schematic of shock impingment.

($S_0 - S_i$). This is proportional to the logarithm of the total pressures $\ln(P_{ti}/P_{t0})$. The importance of the actual flow conditions and geometry on the correlation is also indicated, inasmuch as the entropy levels are critically dependent on shock strength. Such factors as boundary-layer transition and displacement effects could become very important in determining the regions and magnitudes of heating.

The first measurements were obtained for two-dimensional shock impingement, where the local flow properties are constant normal to the wedge body surface. The angle of attack was systematically varied to provide a range of relative shock strengths and the entropy correlation parameter. The effect of sweep on the fin heating was small (a reduction in stagnation line heating of 6% or less over the range of α tested). For the conditions tested, heating on the fins was always for laminar flow conditions. The measured heat-transfer coefficients were compared with Eckert's reference temperature method[3] in the case of the wedge fins, and with a modified Fay and Riddell theory[4] in the case of stagnation-line heating on the cylindrical fins.

Correlation of Impingement Heating

The results of the analysis and initial correlation of the data for both configurations are presented in Fig. 2. It is

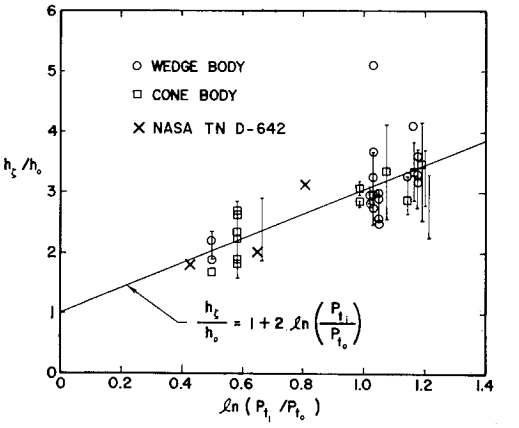

Fig. 2 Heat-transfer rates at shock impingement.

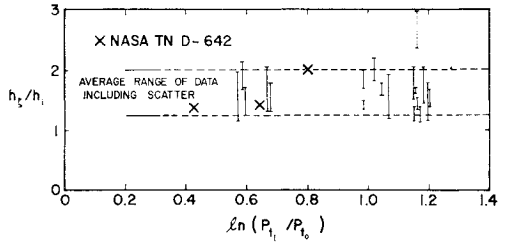

Fig. 3 Correlation of heat-transfer rates at shock impingement.

seen immediately that the nondimensional heat-transfer coefficient ratio h_ζ/h_0 is not constant, but exhibits a variation which is nearly linear. Results from Ref. 5 are also shown and are in good agreement with the present values. Impingement heating rates for body expansion shock waves (at negative α) are not shown. The calculation of the correlation parameter includes the effects of α and fin sweep on the shock angles. It was found that $\ln(P_{ti}/P_{t0})$ is very sensitive to small changes in shock angles and affects the results accordingly. As an example, the initial determination of the correlation parameter for the wedge fins gave results in considerable disagreement with the results for the cylindrical fins. An analysis to include leading-edge and boundary-layer displacement effects on the wedge fin shock angles gave a possible range of the correlation parameters such that agreement with Fig. 2 could be obtained, depending on the assumptions made. This uncertainty raises many questions which have not been solved. The results for the wedge fins have been plotted arbitrarily at the same value of $\ln(P_{ti}/P_{t0})$ obtained for the cylindrical fins (slightly offset in Fig. 2 to indicate the data). Substantial agreement is obtained by this means. The question of a valid correlation is further accentuated by the following apparent anomaly in the variation of $\ln(P_{ti}/P_{t0})$ with α: the correlation parameter passed through a maximum at α between 10° and 15°. The variation of h_ζ/h_0 with $\ln(P_{ti}/P_{t0})$ would thus not necessarily be identical with that due to α; the variation of h_ζ/h_0 with α was approximately linear, within the data scatter.

It is true that the effects of α are to produce a range of relative shock strengths and of the correlation parameter. It is also true, however, that increasing α gives a constantly increasing entropy level inside the body shock. Since the heat-transfer rates can be specified as a function of the entropy magnitude, the possibility exists that the impingement heating could vary as some function of the entropy level as well as the local gradient that produces a region of high vorticity. The predicted heat-transfer rates inside the body shock can be shown to be much higher than those outside and to exhibit increasing values as α increases. The correlation in Fig. 3 was then made to show the variation of h_ζ/h_i vs $\ln(P_{ti}/P_{t0})$. This shows h_ζ/h_i to be approximately constant, where $1.4 < h_\zeta/h_i < 2.0$. It thus appears that the variation in peak heating at impingement as depicted in Fig. 2 is not a variation due to the vorticity effects, but rather due to α.

Concluding Remarks

It is implied from the experimental results that the increased local heating exhibits no discernible variation with shock strength (i.e., M) or Re in the experimental range. The distributions of heating on the fins away from impingement agree reasonably well with current simple methods of prediction. Since the region affected by shock impingement is very localized on the geometries tested, this means that, for application to similar shock-impingement cases where the vehicle may be very large, the thermal protection required for the impingement area may be quite small in comparison to the total thermal protection required.

References

[1] Ferri, A., *Elements of Aerodynamics of Supersonic Flows* (The Macmillan Co., New York, 1949), Chap. 4, pp. 73–74.

[2] Hoshizaki, H., "Mass transfer and shock generated vorticity," ARS J. **30**, 628–634 (1960).

[3] Eckert, E. R. G., "Survey of boundary-layer heat transfer at high velocities and high temperatures," Wright Air Development Center TR 59-624 (1960).

[4] Fay, J. A. and Riddell, F. R., "Theory of stagnation point heat transfer in dissociated air," J. Aerospace Sci. **25**, 73–85, 121 (1958).

[5] Newlander, R. A., "Effect of shock impingement on the distribution of heat-transfer coefficients on a right circular cylinder at Mach numbers of 2.65, 3.51, and 4.44," NASA TN D-642 (January 1961).

An Improved Technique for Obtaining Quantitative Aerodynamic Heat-Transfer Data with Surface Coating Materials

ROBERT A. JONES* AND JAMES L. HUNT†
NASA Langley Research Center, Hampton, Va.

Nomenclature

A = temperature at which phase change occurs
$\hat{A}$ = temperature condition $(A - T_i)/(T_{aw} - T_i)$
h = aerodynamic heat-transfer coefficient, h_0 = reference value for a sphere of radius equal to model base radius, h_s = stagnation-point value
k = thermal conductivity
l = allowable depth of heat penetration
M_∞ = freestream Mach number
p = parameter $(h/k)(\alpha t)^{1/2}$
r = spherical radius
$P_{\infty,D}$ = freestream Reynolds number based on maximum model diameter
t = time, t_d = thermal diffusion time
T = temperature, T_{aw} = adiabatic wall temperature, T_i = initial temperature of model
x = distance normal to back surface of bell-shaped configuration along axis of symmetry
y = distance normal to model surface
α = thermal diffusivity

Introduction

IN Ref. 1 a method for obtaining quantitative aerodynamic heat-transfer data by the use of a visible phase-change coating is described briefly. The coating materials‡ undergo a phase change from an opaque solid to a clear liquid at known temperatures with an accuracy of ±1% which is independent of both ambient pressure and heating rate.† This note further discusses the accuracy of this method and presents additional experimental results.

Technique

The phase-change time patterns are recorded by motion-picture photography with precise framing rates. A transient heat-transfer technique is used whereby the tunnel is brought to the desired stagnation conditions, and the camera is started before the model is injected into the test section. The injection time (the time from which the model first encounters

Presented as Preprint 65-131 at the AIAA 2nd Aerospace Sciences Meeting, New York, N. Y., January 25–27, 1965; revision received April 9, 1965.

* Aerospace Engineer. Member AIAA.
† Aerospace Engineer. Associate Member AIAA.

‡ The phase-change materials used are called Tempilaq and are sold by the Tempil Corporation of New York.